The molecular tweezer CLR01 reduces aggregated, pathologic, and seeding-competent α-synuclein in experimental multiple system atrophy

Marcos Herrera-Vaquero[a,1], Danielle Bouquio[b,c,1], Martin Kallab[a], Karl Biggs[b], Gayatri Nair[b], Jessica Ochoa[b,d], Antonio Heras-Garvin[a], Christian Heid[e], Inesa Hadrovic[e], Werner Poewe[a], Gregor K. Wenning[a], Frank-Gerrit Klärner[e], Thomas Schrader[e], Gal Bitan[b,d,**], Nadia Stefanova[a,*]

[a] Division of Neurobiology, Department of Neurology, Medical University of Innsbruck, Austria
[b] Department of Neurology, David Geffen School of Medicine, University of California, Los Angeles, CA, USA
[c] Department of Molecular and Medical Pharmacology, David Geffen School of Medicine, University of California, Los Angeles, CA, USA
[d] Brain Research Institute and Molecular Biology Institute, University of California, Los Angeles, CA, USA
[e] Institute of Chemistry, University of Duisburg-Essen, Essen, Germany

ARTICLE INFO

ABSTRACT

Multiple system atrophy (MSA) is a fatal, adult-onset neurodegenerative disorder that has no cure and very limited treatment options. MSA is characterized by deposition of fibrillar α-synuclein (α-syn) in glial cytoplasmic inclusions in oligodendrocytes. Similar to other synucleinopathies, α-syn self-assembly is thought to be a key pathologic event and a prominent target for disease modification in MSA. Molecular tweezers are broad-spectrum nanochaperones that prevent formation of toxic protein assemblies and enhance their clearance. The current lead compound, CLR01, has been shown to inhibit α-syn aggregation but has not yet been tested in the context of MSA. To fill this gap, here, we conducted a proof-of-concept study to assess the efficacy of CLR01 in remodeling MSA-like α-syn pathology in the PLP-α-syn mouse model of MSA. Six-month-old mice received intracerebroventricular CLR01 (0.3 or 1 mg/kg per day) or vehicle for 32 days. Open-field test revealed a significant, dose-dependent amelioration of an anxiety-like phenotype. Subsequently, immunohistochemical and biochemical analyses showed dose-dependent reduction of pathological and seeding-competent forms of α-syn, which correlated with the behavioral phenotype. CLR01 treatment also promoted dopaminergic neuron survival in the substantia nigra. To our knowledge, this is the first demonstration of an agent that reduces formation of putative high-molecular-weight oligomers and seeding-competent α-syn in a mouse model of MSA, supporting the view that these species are key to the neurodegenerative process and its cell-to-cell progression in MSA. Our study suggests that CLR01 is an attractive therapeutic candidate for disease modification in MSA and related synucleinopathies, supporting further preclinical development.

1. Introduction

Multiple system atrophy (MSA) is a fatal, adult-onset neurodegenerative disorder, clinically presenting with a combination of motor, autonomic, and often cognitive symptoms [1]. MSA is characterized neuropathologically by the deposition of fibrillar α-synuclein (α-syn) in glial cytoplasmic inclusions (GCIs) in oligodendrocytes [2]. Similar to other synucleinopathies, α-syn self-assembly is thought to be a key pathologic event [3] and therefore, it is a prominent target for disease modification in MSA. Recent pre-clinical studies have supported the efficacy of strategies targeting α-syn oligomerization and aggregation in MSA transgenic models. Among those have been agents preventing

the C-terminal truncation of α-syn [4], aggregation inhibitors [5], and immunotherapies targeting candidate pathogenic epitopes of α-syn [6]. These strategies depend on the presence of specific forms of α-syn, which may or may not be present in the brain of individuals afflicted with MSA. Therefore, broad-spectrum agents targeting all pathological forms of α-syn are of high interest. Furthermore, clinical overlap between MSA and other synucleinopathies, including Parkinson's disease (PD) and dementia with Lewy bodies (DLB), often leads to misdiagnosis [7]. Therefore, compounds that act inclusively against all synucleinopathies may have significant advantages in clinical practice.

Molecular tweezers are broad-spectrum nanochaperones that prevent formation of toxic protein oligomers and aggregates and enhance their clearance by disrupting the interactions that mediate formation of these species and stabilizing non-toxic and non-amyloidogenic structures [8,9]. They achieve this activity by binding selectively to positively charged amino-acid residues, primarily Lys, thereby interfering with a combination of hydrophobic and electrostatic interactions mediating the early stages of aberrant protein self-assembly. The molecular tweezers achieve selectivity through moderate binding affinity and a preference for solvent-exposed residues, which are abundant in unstructured proteins. This allows them to prevent formation of toxic protein assemblies held together by relatively weak forces, such as oligomers and aggregation nuclei of amyloidogenic proteins, without interfering with the structure or function of normal proteins [9].

The current lead molecular tweezer, CLR01 (Fig. 2A), has been shown to inhibit α-syn aggregation *in vitro* by binding to Lys residues primarily at the N-terminus of the protein [10,11]. CLR01 protected cultured PC12 cells against the toxicity of exogenously added α-syn oligomers and α-syn expressed endogenously in the cells [12]. *In vivo*, CLR01 was found to inhibit aggregation, facilitate clearance of toxic assemblies, and ameliorate the pathologic phenotype in zebrafish [12,13] and lamprey [14] models. Lastly, in a PD mouse model expressing human, wild-type α-syn under the neuronal Thy1 promoter, treatment with CLR01 improved motor deficits and reduced soluble α-syn [15]. However, CLR01 has never been tested in a model of MSA. In view of recent studies demonstrating that α-syn in MSA is conformationally distinct and perhaps more pathogenic than in PD [3], it is important to test whether compounds targeting α-syn self-assembly, such as CLR01, could be used as therapeutic agents not only in PD but also in MSA. Here, we conducted a proof-of-concept study to assess the efficacy of CLR01 in remodeling MSA-like α-syn pathology in a transgenic mouse model of MSA. We demonstrate that the treatment improved an anxiety-like behavior in correlation with reducing GCIs and other pathological forms of α-syn. We also show that CLR01 treatment decreases α-syn seeding in a biosensor-cell assay that shows promise for monitoring target engagement in drug-testing studies for synucleinopathies.

2. Results

2.1. CLR01 reverses an anxiety-like phenotype of PLP-α-syn mice

Because in MSA α-syn pathology accumulates in oligodendrocytes as opposed to neurons in PD and there are no data on whether CLR01 can get internalized in oligodendrocytes or affect GCIs we considered it prudent to test first if the compound affected α-syn in the MSA mouse model when administered intracerebroventricularly (ICV). In addition, to begin to address whether molecular tweezers can be internalized in oligodendrocytes, we treated the oligodendrocyte cell line HOG with a novel, fluorescently labeled molecular tweezer derivative, CLR16, in which one of the phosphate groups is attached to a TAMRA (5-carboxytetramethylrhodamine) fluorophore (Fig. 1A). Following 8 h of incubation, the molecular tweezer was observed as puncta inside the cells (Fig. 1B) supporting the internalization of the molecular tweezer in oligodendrocytes and justifying further *in vivo* analysis.

Transgenic PLP-α-syn mice expressing human, wild-type α-syn

under the proteolipid protein (PLP) promoter in oligodendrocytes received unilateral, continuous infusion of 0.3 or 1.0 mg/kg per day CLR01 or vehicle (saline) ICV for 32 days using osmotic minipumps. The administered doses were substantially higher than those used previously in a PD mouse model [15], raising a concern whether these high doses would be still safe. Encouragingly, we observed no significant mortality, morbidity, changes in appearance, or body weight loss in any treatment group (Fig. 2B, C), suggesting that administering up to 1.0 mg/kg per day CLR01 ICV for 32 days was safe. Two mice in the low dose group died shortly after the beginning of the treatment (Fig. 2B), likely from complications of the surgery required for implanting the osmotic pump and cannula. Because both mice were in the low-dose group, these deaths do not appear to be related to the CLR01 treatment.

Monitoring the mice in the open-field test, we confirmed the lack of measurable motor deficits [16] in this test as evidenced by similar horizontal (Fig. 2D) and rearing activity (Fig. 2E) among all the groups. However, we observed a significant anxiety-like behavior in vehicle-treated PLP-α-syn mice, reflected by a lower amount of time spent in the center of the field relative to the periphery, compared to age- and sex-matched non-transgenic control mice (Fig. 2F). Therefore, we tested if treatment with CLR01 could improve this anxiety-like phenotype. Indeed, treatment of the PLP-α-syn mice with 0.3- or 1.0-mg/kg per day CLR01 resulted in a significant, dose-dependent amelioration of this phenotype, which in the high-dose group was statistically indistinguishable from the wild-type control group (Fig. 2F).

2.2. CLR01 decreases GCIs dose-dependently in the PLP-α-syn mouse brain

In view of the therapeutic effect of CLR01 on the anxiety-like behavior of the treated mice, we asked next how this effect was related to changes in pathological forms of α-syn in the brain of the treated mice. The hemisphere contralateral to the ICV cannula in each mouse brain was used for immunohistochemistry applying the monoclonal antibodies ab51253, which detects α-syn phosphorylated at Ser129 (pS129-α-syn) [16], and 5G4, which detects aggregated α-syn [17,18], to identify GCIs in the brains of the mice.

The number of GCIs per area was quantified in brain regions located at different bregma levels and distances relative to the infusion cannula (anterior or posterior). We analyzed striatum, prefrontal cortex (PFCx), commissura anterior (CA) and corpus callosum (CC) at bregma distance 1.60 mm anterior to the cannula. The striatum also was assessed at 0.52 mm anterior, and at 0.84 mm caudal to the cannula. In the latter position we also assessed the basolateral amygdala (BLA). Finally, further caudally, at a 2.66-mm bregma distance from the cannula we analyzed the density of GCIs in the substantia nigra pars compacta (SNc) and substantia nigra pars reticulata (SNr), and at 3.5 mm, in the pontine nuclei (PN).

pS129- is a common marker of pathological α-syn aggregates [19]. We found abundant pS129-α-syn-positive aggregates in multiple brain regions, as shown previously in the PLP-α-syn mouse model [16]. In agreement with the improvement in the anxiety-like phenotype, we found a significant reduction in the density of pS129-α-syn-positive GCIs in the striatum, BLA, PFCx, CA, CC and SNr of MSA mice in the high-dose group relative to mice who received vehicle (Fig. 3). The effect of CLR01 treatment was lower in regions more distant from the infusion cannula, such as the PN and SNc, suggesting that diffusion of the compound in the brain was limited. The treatment effect was dose-dependent, as the mice in the low-dose group had significantly reduced density of pS129-α-syn-positive GCIs only in regions closer to the infusion cannula, such as the striatum, CA, and PFCx and in these regions, the reduction in GCIs was lower than in the high-dose group (Fig. 3). CLR01-induced reduction of GCI density in the brains of the PLP-α-syn mice also was confirmed using the anti-aggregated α-syn mAb 5G4 (Suppl. Fig. S1).

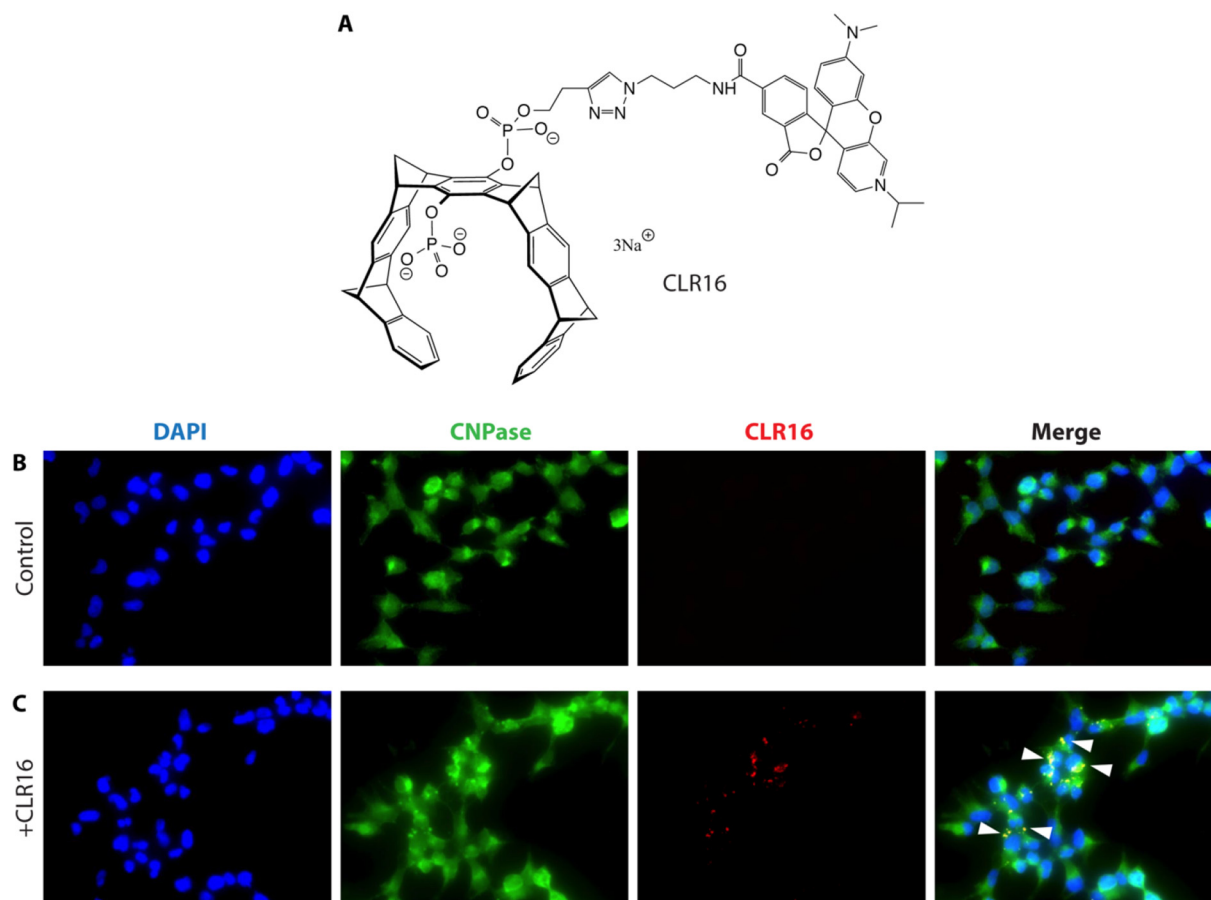To test whether the reduction of GCI density was related to the

Fig. 1. Internalization of CLR16 in oligodendrocytes. A) Schematic structure of the TAMRA-labeled molecular-tweezer derivative, CLR16. B,C) Human oligoden-droglioma (HOG) cells were incubated for 8 h in the absence (B) or presence (C) of 5 μM CLR16, co-stained for DAPI (nuclei) and the oligodendrocyte marker, CNPase, and imaged using a fluorescence microscope. White arrowheads in the merged images on the right indicate the location of CLR16 within oligodendrocytes.

improvement in the anxiety-like behavior, we compared the two parameters across all three treatment groups. A linear-regression analysis showed that the reduction in the density of GCIs in PFCx, BLA, and CA correlated significantly with the reversal of the anxiety-like phenotype (higher Center:Periphery ratio, Fig. 4). Similar data were obtained with mAb 5G4 (Suppl. Fig. S1).

2.3. CLR01 treatment reduces high-molecular-weight pS129-α-syn species

The ipsilateral hemisphere was dissected into five regions of interest, including brainstem, cerebellum, midbrain, hippocampus, and forebrain. Each region was flash frozen and later used for biochemical and seeding analyses. Extraction was performed in two steps – first using tris-buffered saline (TBS) to extract soluble proteins (soluble fraction), and then using TBS containing 1% Triton X-100 and 5 M guanidine to extract insoluble proteins (insoluble fraction).

Western blot analysis using the pS129-α-syn-specific mAb MJF-R13 [8] showed predominantly a phosphorylated monomer in the soluble fraction, whereas both a monomer and a high-molecular-weight band (~90 kDa) were detected in the insoluble fraction (Fig. 5A and Supplemental Fig. S2A). For quantification, the densitometric value of the bands was measured and normalized first to Ponceau S staining of the entire lane as a loading control and then to total α-syn, which was measured by ELISA. Though the same bands were observed in the different brain regions, the quantitative analysis showed a high variability, likely due both to the normal variability among mice and to the uneven distribution of CLR01 in the brain. Therefore, the values for the different brain regions were combined for each mouse to calculate the normalized abundance of pS129-α-syn in the whole brain.

The densitometric analysis showed that the treatment did not affect the phosphorylated monomer in the soluble fraction (Fig. 5B). In contrast, in the insoluble fraction, the abundance of both the monomer and the HMW band were reduced dose-dependently by the treatment (Fig. 5C,D). The decrease in the HMW band (Fig. 5G), but not the monomer band in either fraction (Fig. 5E,F), correlated significantly with the improvement in the anxiety-like behavior, suggesting that it represented a toxic form of α-syn.

In view of the known mechanism of action of CLR01—inhibition of self-assembly of amyloidognic proteins, a likely consequence of the decrease in pS129-α-syn concentration levels in the insoluble fraction would be an increase of this form of α-syn in the soluble fraction,. However, we did not observe such an increase (Fig. 5B). One possible explanation is that soluble α-syn exists more in an unphosphorylated form, as opposed to the enrichment in pS129-α-syn in GCIs. In support of this idea, we found a significant, dose-dependent increase in total α-syn in the soluble fraction (Fig. 6A), but not in the insoluble fraction (Fig. 6B).

2.4. CLR01 treatment decreases putative high-molecular weight α-syn oligomers

The main effect of CLR01 on α-syn in vitro has been shown to be remodeling of oligomers into non-toxic and non-amyloidogenic structures [11,12]. The observation of reduced HMW pS129-α-syn was in line with this meachanism, yet SDS-PAGE is not a reliable method for analyzing oligomers of amyloidogenic proteins, such as α-syn [20]. Therefore, to assess whether CLR01 affected the abundance and/or size distribution of α-syn oligomers in the brain of the PLP-α-syn mice, we
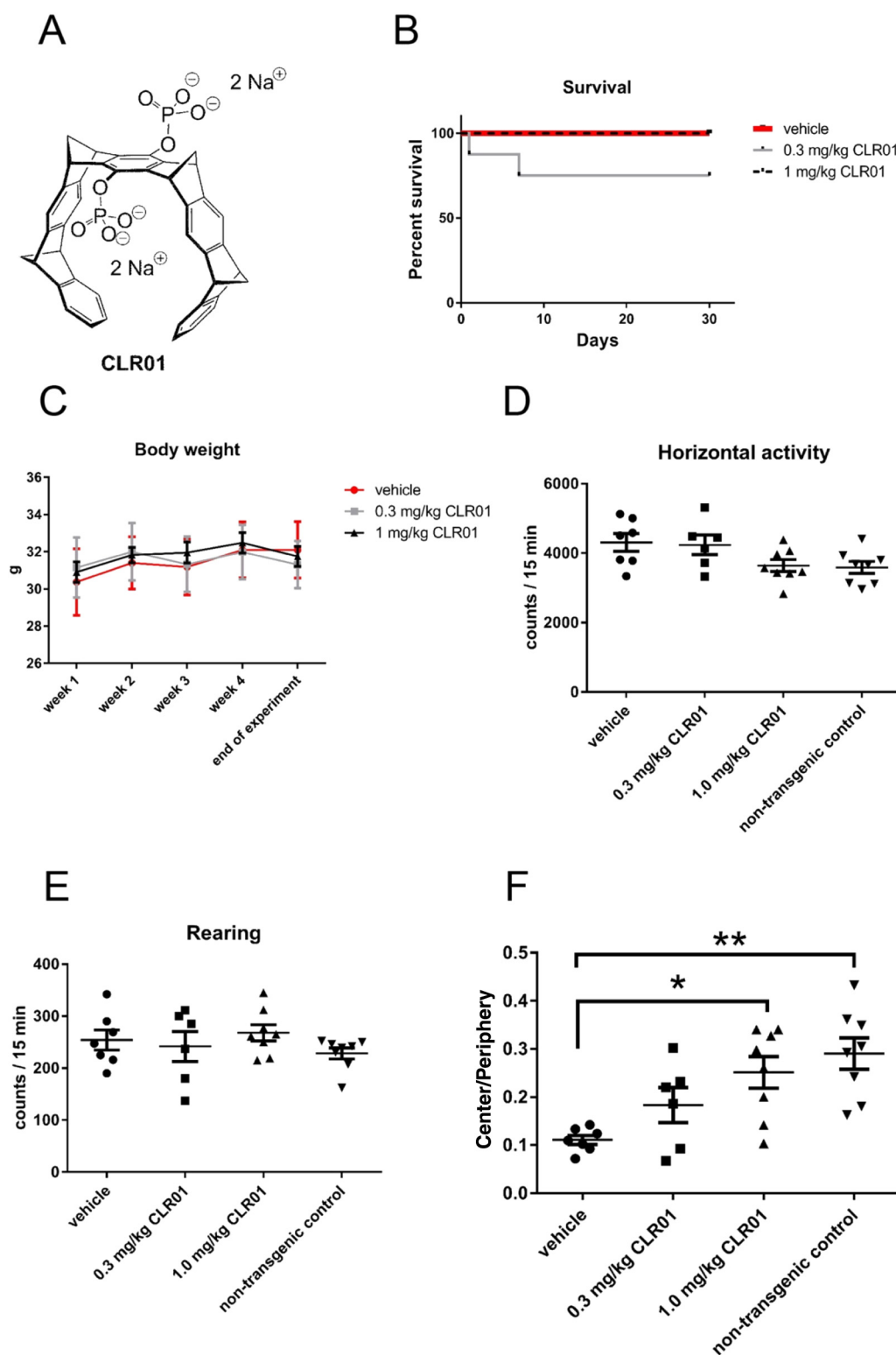
Fig. 2. CLR01 treatment is safe and rescues an anxiety-like behavior of PLP-α-syn mice. A) A schematic structure of CLR01. The compound is partially protonated at physiologic pH. B) A survival curve for the mice used in the study. C) Body-weight change during the treatment period. D,E) Horizontal (D) and rearing (E) locomotor activity of the PLP-α-syn mice receiving CLR01 or vehicle. (F) Ratio between the time spent in the center versus the periphery in the open-field test by PLP-α-syn mice treated with CLR01 or vehicle, and age- and sex-matched wild-type controls. Data are presented as mean ± SEM. *$p < 0.05$, **$p < 0.01$ (one-way ANOVA with post hoc Bonferroni test).

analyzed the soluble fraction using Blue native PAGE/western blot probed with the anti-α-syn mAb MJFR1. Interestingly, the analysis showed that α-syn comprised a series of bands consistent with oligomers, in which putative dimer through pentamer/hexamer could be resolved, and higher molecular weight species appeared as a smear (Fig. 7A and Supplemental Fig. S2B).

Because in native PAGE proteins do not separate simply according to size as they do in SDS-PAGE, it is difficult to determine the molecular weight of the proteins based on their apparent electrophoretic mobility,

even using protein standards. Therefore, to assess the molecular weight of the bands, we used recombinant α-syn cross-linked using Photo-Induced Cross-linking of Unmodified Proteins (PICUP) [21,22]. Previously, SDS-PAGE analysis of α-syn cross-linked by PICUP showed that oligomers up to a hexamer could be discerned [11,23]. The brain extract putative monomer actually appeared as two separate bands – one with a slightly faster mobility than the recombinant monomer (either cross-linked or not, (Fig. 7A), which we termed monomer-low) and the other with a slower mobility (monomer-high). These bands may
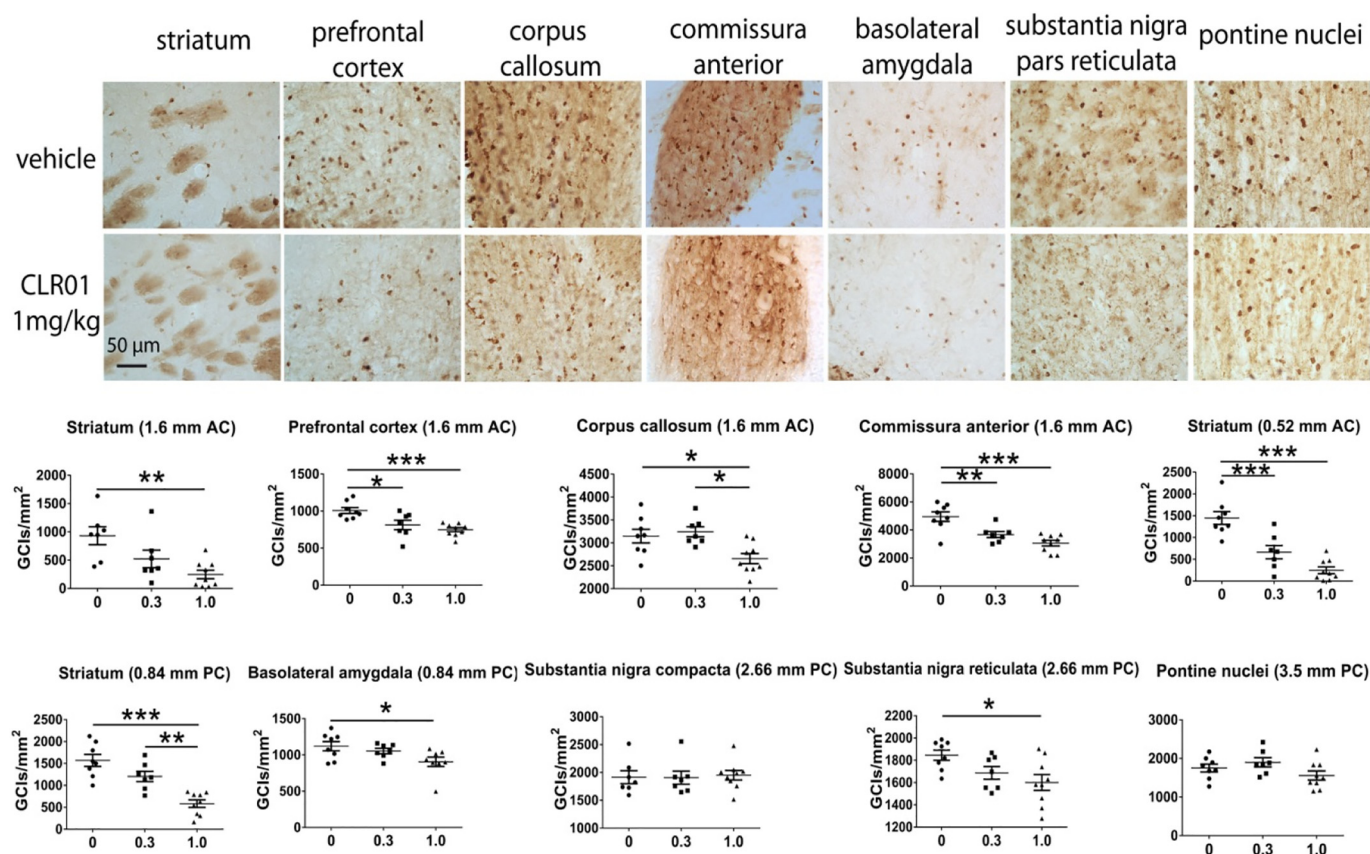
Fig. 3. CLR01 treatment reduces in a dose-dependent manner the density of GCIs in PLP-α-syn mouse brains. GCI density was studied in brain sections stained for phosphorylated α-syn (pS129). Several regions positioned at variable distances anterior to the infusion cannula (AC) or prosterior to the cannula (PC) were assessed. Data are presented as mean ± SEM and analyzed by one-way ANOVA with post hoc Bonferroni test. *$p < 0.05$, **$p < 0.01$, ***$p < 0.001$.
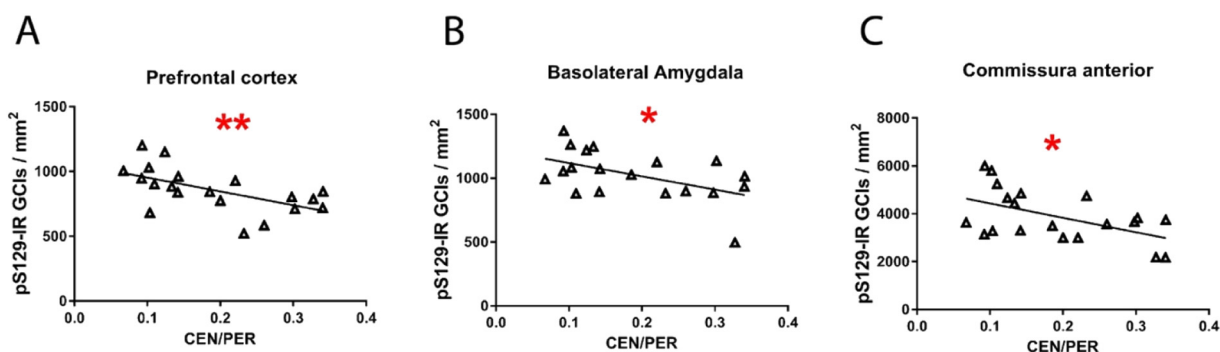

Fig. 4. The reduced density of GCIs in PLP-α-syn mouse brains correlates with the improvement of the anxiety-like behavior after CLR01 treatment. (A) Prefrontal cortex, $r^2 = 0.34$, $p = 0.007$. (B) Basolateral amygdala, $r^2 = 0.26$, $p = 0.03$. (C) Commissura anterior, $r^2 = 0.28$, $p = 0.02$.

represent two different conformers of α-syn, post-translational modifications, truncations, and/or non-covalent association of α-syn with other biomolecules. The electrophoretic migration of the bands in the brain extracts, which were not cross-linked, was consistently slower than that of the cross-linked, recombinant α-syn (Fig. 7A).

The most plausible explanation for this behavior is binding of α-syn oligomers in the brain extracts to an unknown component, likely lipid molecules. However, testing this hypothesis is highly challenging because the bands in the extract represent non-covalent complexes and manipulation of these extracts likely would lead to dissociation of the complexes. Excising the bands from the gel, eluting the proteins, and analyzing them by mass-spectrometry was considered but deemed to have a low likelihood of success. The oligomers are likely to dissociate during elution and/or transition to the gas phase in the mass

spectrometer, and many other proteins in the brain extract would be present in each gel band, complicating the analysis. Thus, attempting to test in this way the hypothesis that α-syn molecules in non-covalent oligomers were bound to lipids (or other molecules) was beyond the scope of this study. Because we could not formally rule out the possibility that the bands in the brain extracts represented α-syn monomer bound to other biomolecules, we designated these bands putative oligomers.

The observation of putative oligomers up to a hexamer was in contrast to a similar analysis in Thy1-aSyn mice, in which the only resolved bands were monomer and putative dimer, whereas all higher-order species migrated together as one smear [15]. At this point, it is not known if the distinct putative oligomer patterns in the two studies represent genuine differences between α-syn conformations in the brain
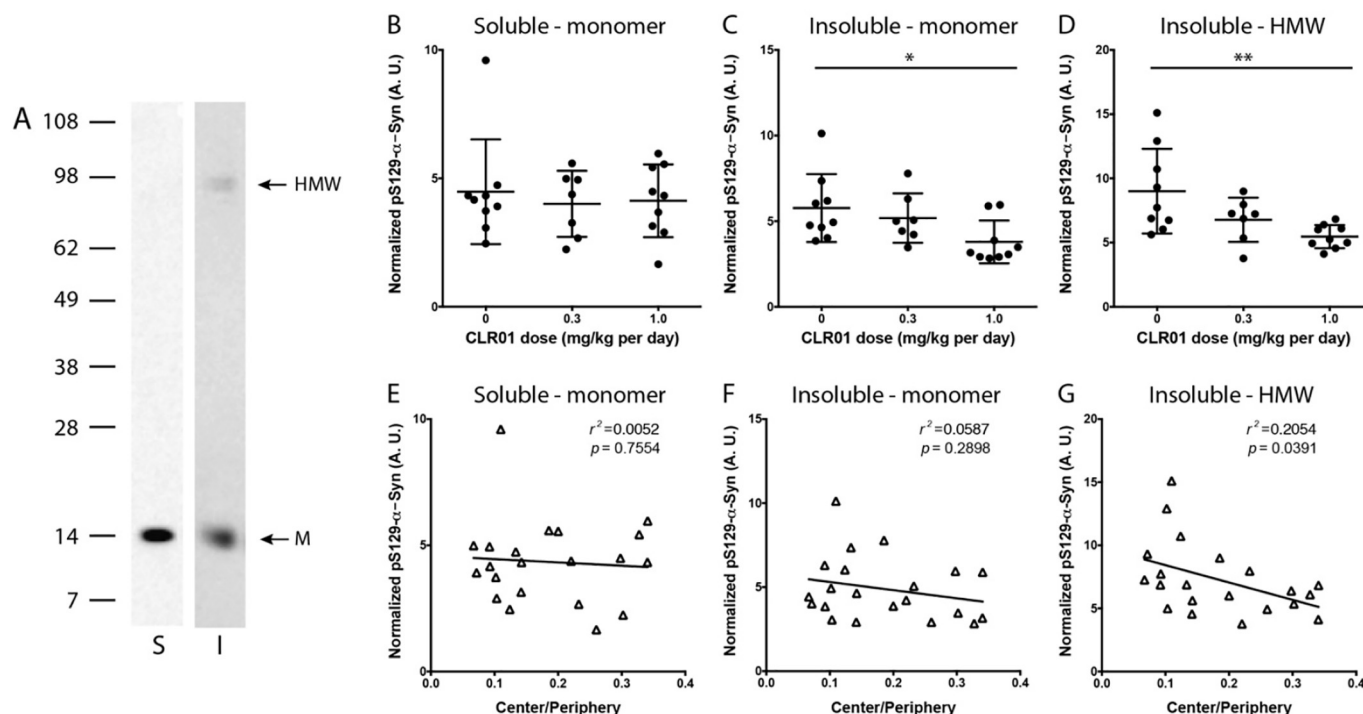
Fig. 5. Western blot analysis of pS129-α-syn. Brain extracts were fractionated by SDS-PAGE and probed by western blot for pS129-α-syn using mAb MJF-R13 [8]. A) Representative blots of midbrain extracts – soluble and insoluble fraction. S = soluble, I = insoluble, M = monomer, HMW = high-molecular-weight band. B–D) Densitometric analysis of the pS129-α-syn monomer in the soluble fraction (B) and insoluble fraction (C), and the HMW band in the insoluble fraction (D) normalized to total α-syn in each fraction. The error bars indicate SD. *$p < 0.05$, ***$p < 0.001$. 1-Way ANOVA with *post-hoc* Tukey test. E-G) Linear regression analysis of the correlation between the normalized pS129-α-syn bands analyzed in panels B-D, respectively and the Center/Periphery ratio.

of PD and MSA mouse models or stemmed from technical differences between the two studies. It will be interesting to address this question in future studies.

To determine if the treatment affected the putative oligomer size distribution, we used densitometry to analyze each of the bands, including the two apparent monomer bands, the discernable putative oligomers up to a pentamer, and the HMW smear. The putative hexamer band in the brain extracts was not observed consistently in all cases and therefore was not included in the analysis. We attempted to use several loading controls, including α-tubulin, β-actin (two different antibodies), and GADPH (two different antibodies) yet none provided consistent and reliable data. Therefore, each band was normalized to the density of the entire lane in each gel. The densitometric analysis showed a trend towards dissociation of high-molecular weight species

and an increase in α-syn monomer (Fig. 7B). This effect was observed primarily in the high-dose group compared to the mice receiving vehicle, whereas the low-dose group showed variable results (Fig. 7B,C). Overall, the analysis suggested that the behavioral improvement correlated with dissociation of high-molecular-weight species into monomers or small putative oligomers (Fig. 6D). The magnitude of this effect was relatively small, likely because only the soluble fraction could be analyzed. Presumably, dissociation of HMW oligomers would have been more prominent in the insoluble fraction but because the extraction protocol perturbs the α-syn assembly state in this fraction, this hypothesis could not be tested.
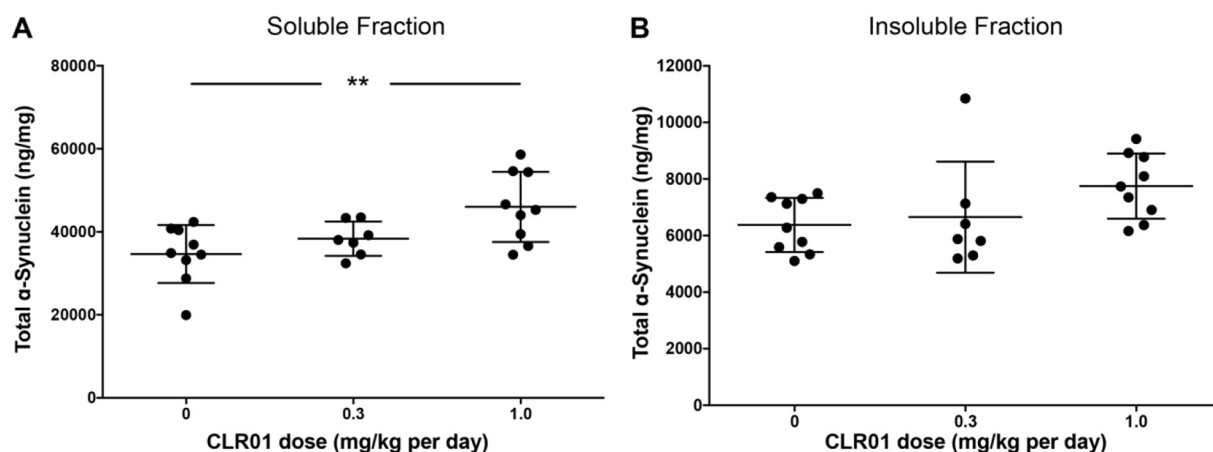

Fig. 6. Effect of CLR01 on total α-syn. The concentration of α-syn in the soluble (A) and insoluble (B) fractions was measured using a commercial ELISA kit. The data are presented as mean ± SEM. **$p < 0.01$, one-way ANOVA with *post-hoc* Tukey test.
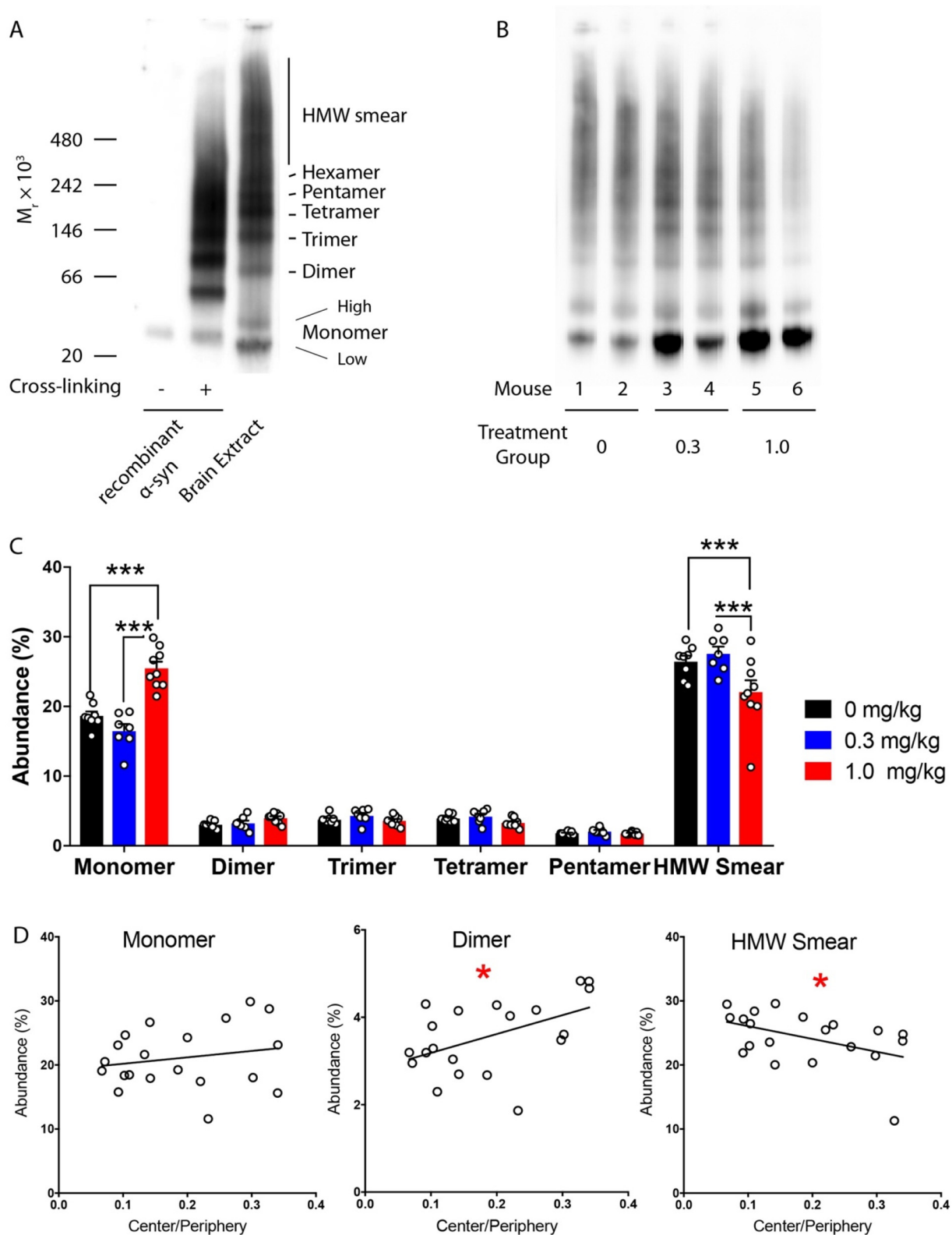
Fig. 7. Native-PAGE/western blot analysis of α-syn in the soluble fraction. The soluble fraction of the mouse brain extracts was fractionated by native-PAGE and probed by western blot using mAb MJFR1. A) a representative blot showing recombinant α-syn, recombinant α-syn cross-linked using PICUP, and a representative midbrain brain extract from one mouse. B) a representative blot showing the different α-syn species in midbrain extracts from the three treatment groups. C) Densitometric analysis of the different bands in the whole brain (calculated as the sum of the different brain regions). The data are presented as mean ± SEM. ***$p < 0.001$, two-way ANOVA with *post-hoc* Tukey test. D) Linear regression analyses of specific α-syn assemblies versus the ratio of the time spent in the center versus the periphery. *$p < 0.05$.
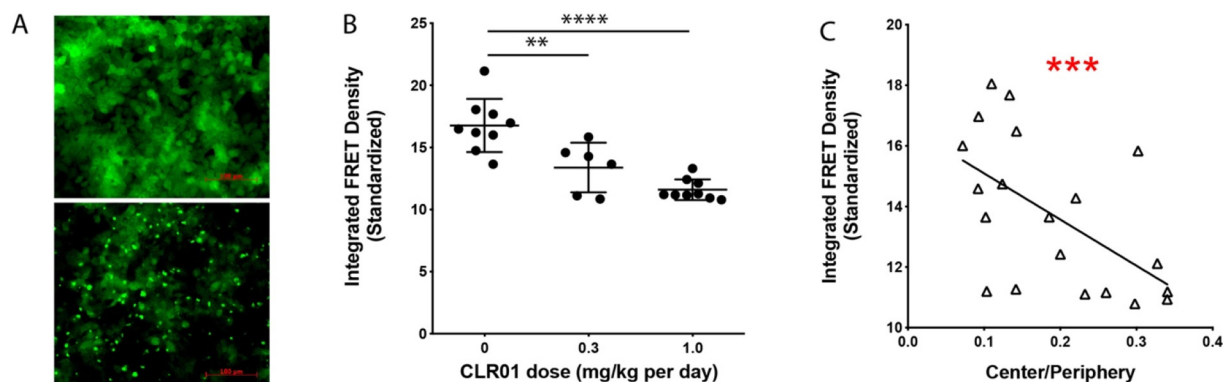
Fig. 8. CLR01 treatment reduces α-syn seeds in MSA mouse brain. A) Examples of unseeded (top) and seeded (bottom) biosensor cells. B) FRET analysis of seed content in the brain extracts' soluble fraction. The error bars indicate SD., **p < 0.01, ****p < 0.0001 one-way ANOVA with *post-hoc* Tukey test. C) Linear regression analysis of the correlation between the seeding activity and the Center/Periphery ratio.

2.5. CLR01 reduces the seeding activity of α-syn in PLP-α-syn mouse brain extracts

Prion-like spreading of α-syn from cell to cell along connected neuronal networks has been an area of intense research in recent years [24]. A particularly intriguing report in this context suggested that extracts from brains of patients with MSA seeded aggregation of α-syn in biosensor, HEK293T cells expressing A53T-α-syn conjugated to yellow fluorescent protein (YFP), whereas brain extracts from patients with PD did not [3]. To assess whether CLR01 treatment affected the seeding capability of α-syn extracted from the brain of the PLP-α-syn mice, we used a different biosensor-cell assay developed by Diamond and co-workers, which employs fluorescence-resonance energy transfer (FRET) between α-syn molecules conjugated to CFP or YFP [25]. Aggregation of α-syn in this assay can be visualized using fluorescence microscopy (Fig. 8A) and is quantified by flow cytometry.

We tested the seeding activity only in the soluble fraction because the presence of the detergent in the insoluble fraction was toxic to the cells. The soluble fraction from each region was analyzed separately yet when analyzing each region separately, the data were difficult to interpret because they reflected both the normal variability among the mice and the limited diffusion of CLR01 from the cannula to different regions of the brain. Therefore, the results of the different regions were added together and presented as the sum of the whole brain. The analysis showed that CLR01 treatment reduced the seeding activity of α-syn significantly and dose-dependently (Fig. 8B). Linear regression analysis showed that this decrease correlated with the improvement in the anxiety-like behavior ($r^2 = 0.323$, $p = 0.009$). It was also of interest to test how the decrease in seeding activity in the soluble fraction correlated with the changes in the species detected by native PAGE in this fraction. Linear regression analysis showed significant correlation between the decrease in seeding activity and an increase in the abundance of monomer ($r^2 = 0.218$, $p = 0.022$) and dimer ($r^2 = 0.178$, $p = 0.040$), but not with changes in abundance of other species.

2.6. CLR01 dose-dependently rescues nigral dopaminergic neurons in the PLP-α-syn mouse brain

Neurodegeneration in the substantia nigra pars compacta (SNc) is a prominent feature of the neuropathology of the PLP-α-syn mouse model at six months of age [16]. To determine if CLR01 treatment affected the dopaminergic neuronal loss in the SNc, we assessed the number of tyrosine-hydroxylase (TH)-positive neurons stereologically in the three treatment groups (Fig. 9A, B). We found that the treatment rescued the dopaminergic neurons significantly in the high-dose group (5469 ± 1327 TH neurons) compared to the control (3603 ± 840) and low-dose (3774 ± 822) groups, a 52% increase in the high-dose

group relative to the vehicle-treated mice.

We asked next if the increase in TH neurons survival correlated with a decrease with putative toxic α-syn oligomers. Linear-regression analysis showed a significant correlation between the rescue of TH neurons in the SNc, the decreased abundance of the putative high-molecular weight oligomers ($r^2 = 0.192$, $p = 0.032$, Fig. 9C), and the increased abundance of monomer ($r^2 = 0.226$, $p = 0.019$, Fig. 9D) detected by native PAGE, supporting the notion that the putative HMW oligomers represented major toxic species.

3. Discussion

The current study provides for the first-time evidence for the efficacy of the molecular tweezer CLR01 in a mouse model of MSA. The continuous ICV administration of CLR01 in PLP-α-syn mice resulted in a dose-dependent rescue of the anxiety-like phenotype (Fig. 2E), a reduction of the intracellular accumulation of α-syn in GCIs (Fig. 3), the pathological hallmarks of MSA, and a rescue of dopaminergic neurons in the SNc (Fig. 9). Biochemical analysis showed that the process by which CLR01 lowered GCIs likely involved remodeling of α-syn conformation, as was reported previously in vitro [11], reducing pathological pS129-α-syn in the insoluble fraction (Fig. 5) and increasing the levels of soluble total α-syn (Fig. 6). In agreement with these results, the treatment promoted a shift from high-molecular weight species towards low-molecular weight putative oligomers and monomers (Fig. 7) and reduced α-syn seeds dose-dependently in the PLP-α-syn mouse brain (Fig. 8). The shift from high-molecular weight species towards monomers apparently allowed rescue of degenerating nigral dopaminergic neurons in the MSA mouse brain (Fig. 9).

Previously, CLR01 was shown to prevent α-syn aggregation and dissociate pre-formed α-syn aggregates in vitro [11,12]. This capability of the molecular tweezer has been further demonstrated in several cell-culture and in-vivo models of PD-like synucleinopathy [12,13,15] and spinal-cord injury [14], and was associated with amelioration of specific disease phenotypes. The current findings corroborate these previous observations and support the proposed target engagement of CLR01 in a model of MSA-like oligodendroglial α-synucleinopathy. We demonstrate here for the first time in the context of MSA that CLR01 achieves these beneficial effects by inducing a shift from high-order to low-order putative oligomers and monomeric forms of α-syn. In addition, our data suggest that by inhibiting α-syn aggregation, the protein is shifted from the pathological form phosphorylated at Ser129 in the insoluble fraction to the unphosphorylated, presumably native, soluble form. This latter effect is important not only for prevention of the gain-of-toxic-function mechanism of α-syn, but also for restoring the loss of synaptic α-syn, which may contribute to the pathology in synucleinopathies [27,28].
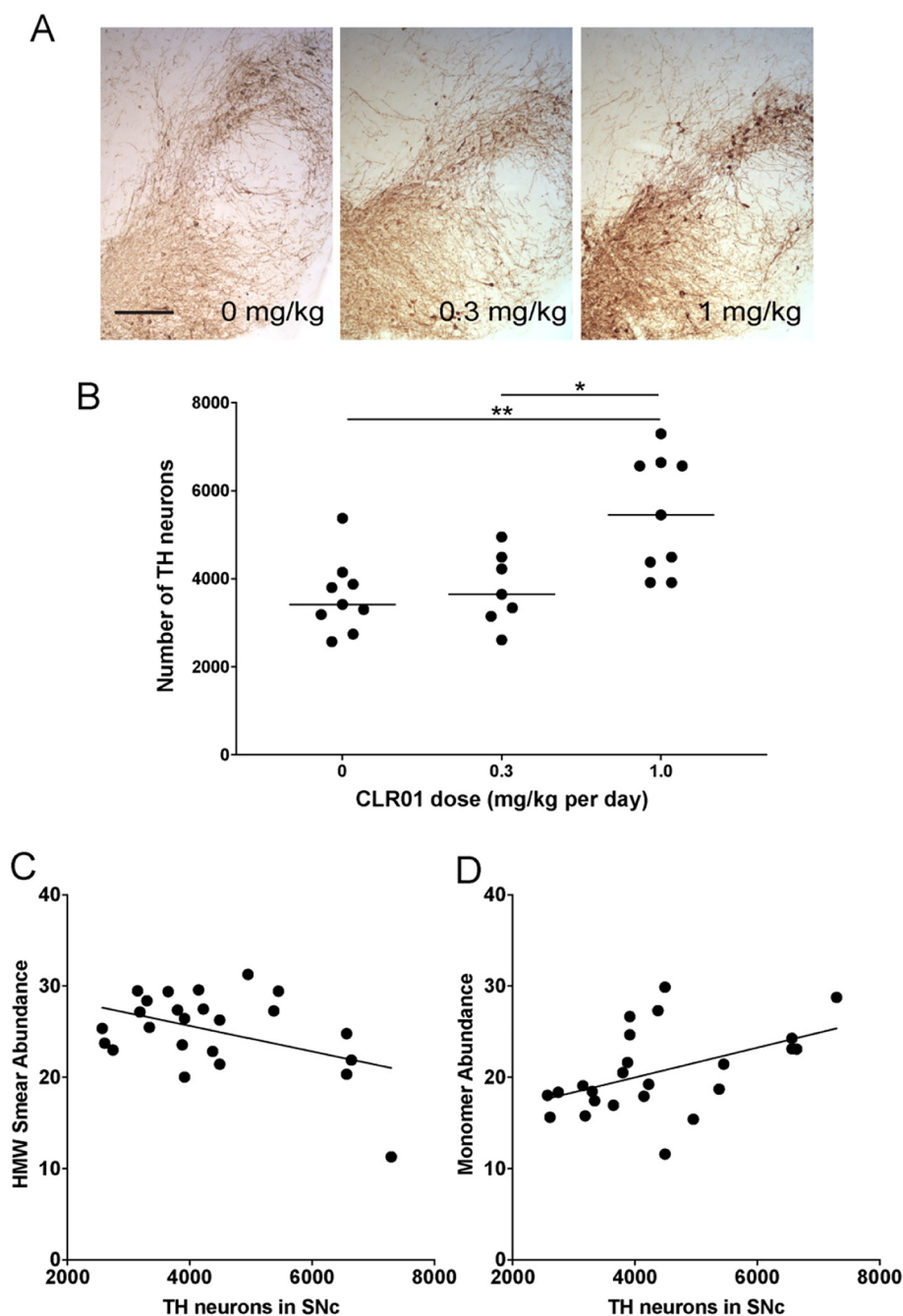
Fig. 9. CLR01 treatment rescues dopaminergic neurons in the SNc of PLP-α-syn mice. A) Representative images of TH immunohistochemistry in the SNc of mice from the three treatment groups, the scale bar represents 400 μm. B) Number of TH-immunopositive neurons in the SNc determined by stereology. *p < 0.05, **p < 0.01 (one-way ANOVA with post hoc Bonferroni test). C) Linear regression analysis of the correlation between the number of TH neurons in SNc and the abundance of putative HMW α-syn oligomers measured in native-PAGE (p = 0.032). D) Linear regression analysis of the correlation between the number of TH neurons in SNc and the abundance of α-syn monomers measured in native-PAGE (p = 0.019).

The results of the native-PAGE and biosensor-cell analyses, and the correlation found between them, suggest that soluble, HMW α-syn species act as seeds, presumably contributing to the spreading of α-syn throughout the brain, and that CLR01 treatment reduces the level of these seeds. Similar cell-based seeding sensor systems have been shown previously to detect the tendency of MSA-derived α-syn to form pathogenic oligomers and aggregates [3]. Our results show that α-syn in brain lysates of PLP-α-syn mice replicate this feature of human MSA and trigger aggregate formation in the biosensor cells. In view of the results obtained here, CLR01 treatment may not only mitigate the toxicity of existing α-syn assemblies in affected mouse and patient brain, but also could decelerate or halt the spread of the pathogenic species throughout the brain. Importantly, the shift from HMW α-syn species to monomers led to neuroprotection of nigral neurons even before the detection of reduction of GCI-like inclusions in the SNc, supporting the early beneficial role of α-syn remodeling through CLR01

treatment on nigral neurodegeneration in the MSA model.

Among the brain structures that showed changes in GCI-like aggregation in the PLP-α-syn brain after treatment with CLR01 were the prefrontal cortex and the basolateral amygdala, involved in the control of anxiety [29]. Indeed, anxiety-like behavior, as measured here in the PLP-α-syn mouse by the preference of periphery to center in an open-field arena, was reduced significantly and dose-dependently by treatment with CLR01. Furthermore, the improvement of the anxiety-like behavior correlated with the lowering of GCIs in the basolateral amygdala, premotor cortex and commissura anterior (regions of the anxiety-control circuit), but not with effects in other brain regions. Our results are supported by previous studies that suggested a role for α-syn oligomers in the induction of anxiety-like behavior in mice [30]. Thus, we conclude that CLR01 treatment in PLP-α-syn mice leads to remodeling of pathologic α-syn species, shifting α-syn from a phosphorylated, insoluble form back to the native, soluble form, leading to

functional improvement of disease-associated phenotypes, supporting the therapeutic potential of the molecular tweezer for MSA and justifying further studies on long-term CLR01 treatment and evaluation of neuroprotection and motor deficits' amelioration in the PLP-α-syn mouse.

The translational value of the current study is strengthened by the fact that anxiety is a common feature in MSA [31,32] and therefore we hypothesize that molecular-tweezer-based therapy will be relevant to the treatment of this disorder. It will be important to test in subsequent studies if the efficacy of CLR01 is limited to non-motor features of the disease or may have beneficial effects on motor disability, which was not tested in this initial study. A limitation of the current study is that using the ICV infusion paradigm, we were unable to get sufficient compound diffusion into the substantia nigra, resulting in lack of changes in the GCI density in this region. Further studies are needed to assess the therapeutic potential of CLR01 delivered peripherally and over longer periods of time for a maximal therapeutic effect on motor and non-motor features and halting neurodegeneration and disease progression in MSA.

Taken together, the data presented here suggest that CLR01 is an attractive therapeutic candidate for disease modification in MSA and related synucleinopathies. As demonstrated previously, CLR01 is a broad-spectrum compound that inhibits the formation of toxic oligomers and aggregates by multiple amyloidogenic proteins. This feature may be particularly important for use as a first-line treatment not only of synucleinopathies, but also of other parkinsonian syndromes, such as progressive supranuclear palsy and corticobasal syndrome, which are tauopathies, because the treatment is expected to be effective also against aberrant tau assemblies [10,33] and does not require precise diagnosis.

3.1. Experimental procedures

3.1.1. Synthesis and characterization of CLR16

In a 25-ml round bottom flask, monobutynyl tweezer X (8 mg, 10 μmol, Scheme 1) and TAMRA azide Y (6 mg, 12 μmol) were dissolved in 2 ml freshly distilled tetrahydrofuran (THF). To this solution, 11.3 μl of diisopropylethylamine were added. Finally, a catalyst solution consisting of 8 mg $CuSO_4 \cdot 5H_2O$ and 13 mg sodium ascorbate in 2 ml H_2O was added and the mixture was stirred for 16 h at room temperature. After quenching with 5 ml 2.5% aqueous HCl, the THF was removed in vacuum. The resulting purple residue was filtered (D4), washed with 3×2 ml 2.5% aqueous HCl, and 2×2 ml water. The crude product was purified by preparative HPLC (RP-18, H_2O/MeCN gradient) to obtain CLR16 (2 mg, 1.5 μmol, 15% yield) as a purple solid.

HRMS; m/z **[M-H]** $^{-}$: 1289.3985 calc., 1289.3993 obs.

^{1}H NMR (600 MHz, DMSO-d_6) δ[ppm] = 2.14–2.33 (m, 10H, H-48, H-49, H-69, H-70), 2.95 (t, J = 6.7 Hz, 2H, H-89), 3.25 (s, 12H, H-32 – H-35), 3.41 (q, J = 6.5 Hz, 2H, H-29), 4.05–4.10 (m, 4H, H-37, H-67, H-46, H-47), 4.13 (q, J = 7.0 Hz, 2H, H-88), 4.28–4.32 (m, 4H, H-38, H-45, H-68, H-79), 4.50 (t, J = 7.0 Hz, 2H, H-31), 6.70–6.81 (m,

4H, H-59, H-60, H-74, H-75), 6.90–7.14 (m, 16H, Tweezer + Tamra-Aryl-H), 7.57 (d, J = 7.9 Hz, 1H, TAMRA-Aryl-H), 8.10 (s, 1H, H-91), 8.31 (dd, J = 7.9, 1.8 Hz, 1H, TAMRA-Aryl-H), 8.70 (s, 1H, TAMRA-Aryl-H), 9.00 (t, J = 5.6 Hz, 1H, H-28).

^{13}C NMR (151 MHz, DMSO) δ[ppm] = 26.79, 29.85, 36.89, 40.05, 40.50, 47.35, 47.94, 48.00, 50.25, 50.27, 65.74, 67.79, 69.02, 96.32, 116.70, 116.76, 116.83, 121.42, 122.94, 124.43, 130.44, 135.91, 140.96, 141.27, 141.59, 142.89, 146.57, 146.64, 146.74, 146.85, 146.94, 146.96, 150.24, 150.28, 157.64, 157.85, 164.81.

3.1.2. Analysis of CLR16 internalization in oligodendroglial cells

HOG human oligodendroglioma cells (SCC163, Merck) were grown in DMEM high glucose (Gibco) supplemented with 10% FBS (Gibco) and 1% penicillin/streptomycin (Gibco). The cells were maintained at 37 °C under a humidified atmosphere with 5% CO_2. HOG cells were exposed to 5 μM CLR16 or vehicle (0.2% DMSO) for 8 h. To analyze the intracellular presence of CLR16, HOG cells on coverslips were immunostained with anti-CNPase antibody (1:500, Abcam) followed by a suitable secondary antibody conjugated to Alexa 488 (1:500, Invitrogen) according to a standard protocol. Nuclear staining was performed with DAPI (1:1000, Sigma-Aldrich) and finally coverslips were mounted on slides with Fluromount-G medium (Southern Biotech) and kept in the dark. Images were acquired using a Leica DMi8 fluorescence microscope.
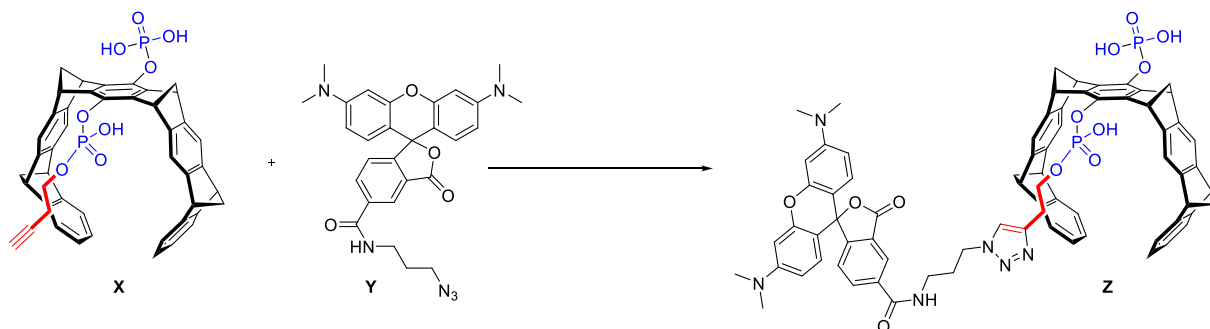
3.1.3. Animals and treatment

Six-months old male homozygous transgenic PLP-α-syn mice (MGI:3604008) overexpressing human α-syn under the PLP-promoter [34] and background-, age- and sex-matched non-transgenic C57Bl/6 mice were used in this study. All animals were bred and housed in a temperature-controlled room under a 12/12-h dark/light cycle, with free access to food and water and under pathogen-free conditions in the animal facility of the Medical University of Innsbruck. All experiments were performed in accordance with the Austrian law under permission BMWFW-66.011/0018-WF/V/3b/2015.

Animals were randomized into three treatment groups, including two doses of CLR01, 0.3 or 1.0 mg/kg per day, or vehicle, which were administered intracerebroventricularly (ICV) by osmotic minipumps (Alzet) over a period of 32 days. The compound was prepared as described previously [35], purified as the sodium salt, and dissolved in sterile saline. The delivery was provided by implanting an ICV cannula into the left lateral ventricle with coordinates AP: −0.5 mm, L: +1.0 mm and V: −2.2 mm to Bregma under deep isoflurane inhalation anesthesia (induction 4%, intra-surgical 1.5%). The tooth bar was set at 0. The cannula was linked to a catheter connected to an Alzet osmotic pump (#1004), which was subcutaneously implanted as described previously [36].

3.1.4. Open-field activity

On day 29 after the initiation of therapy, spontaneous locomotor activity in a 40.5 × 40.5 × 36.5 cm open-field arena was assessed using

Scheme 1. Synthesis of CLR16.

the Flex Field Activity System (San Diego Instruments, San Diego, CA). The measurements were performed in a dark room with noise isolation, between 7 and 9 pm. Total activity, rearing, center activity and thigmotaxis (peripheral activity) of each mouse were recorded for a period of 15 min and used for the comparison of the treatment groups. Center-to-periphery ratio was calculated as a measure of anxiety-like behavior in mice as described previously [29].

3.1.5. Tissue sampling

On day 32, mice were transcardially perfused with 20 ml PBS for 5 min under deep thiopental anesthesia. The brains were removed quickly. The left hemisphere was dissected into sub-regions: forebrain, hippocampus, midbrain, cerebellum, and lower brainstem. Each sub-region was immediately frozen in liquid nitrogen, stored at −80 °C and subsequently used for biochemical analysis. The right hemisphere was immersion-fixed in 4% paraformaldehyde at 4 °C overnight, cryoprotected with 30% sucrose and slowly frozen, stored at −80 °C, and subsequently used for histological analysis.

3.1.6. Histopathology

Fixed hemispheres were cut using a cryotome (Leica, Nussloch, Germany) into 40-µm serial sections. Immunohistochemistry of free-floating sections was performed using standard protocols [16] and the following antibodies: anti-aggregated α-synuclein (5G4, Linaris, Germany, 1:1000), anti-phosphorylated α-synuclein (pS129, ab51253, Abcam, UK, 1:1000), anti-tyrosine hydroxylase (TH, AB152, Millipore, Germany, 1:750), biotinylated anti-mouse, and anti-rabbit IgG (respectively, BA-1000, and BA-2001, Vector Laboratories, US, 1:250). The reaction was enhanced with ABC Elite kit (PK-6100, Vector Laboratories, US) and visualized with 3,3′-diaminobenzidine.

3.1.7. Image analysis

The StereoInvestigator Software (MicroBrightField) was used with a Nikon Eclipse 80i microscope equipped with a motorized stage and a high-resolution digital camera. A low-power objective lens ($2\times$, SPlan) was used to delineate the borders of the areas of interest. Actual object counting was done using a $100\times$-objective (NA 0.75) using the automated meander scan procedure for GCI counting. The data are presented as object density per mm^2. The number of TH-positive neurons in the SNc was determined by stereology using the optical fractionator method as described previously [16].

3.1.8. Tissue extraction

Each brain region was extracted using a modified previously published protocol[15]. Briefly, each brain region was fractionated into a "soluble fraction" (20 mM Tris·HCl, 150 mM NaCl, pH 7.4); and "insoluble fraction" (20 mM Tris·HCl, 150 mM NaCl, 0.1% Triton-X100 and 5 M guanidine hydrochloride, pH 7.4). The latter fraction was desalted using Zeba spin columns (#89882; Thermo Scientific, Waltham, MA, USA). Protein concentration was determined by the BCA assay.

3.1.9. Total α-synuclein ELISA

Novex Human α-Synuclein ELISA kits (ThermoFisher Scientific, catalog number: KHB0061) were used to quantify α-synuclein according to the manufacturer's protocol and using the standard included with the kit. All standards and samples were run in duplicates. Samples showing a coefficient of variation (CV) difference > 20% between measurement were re-run up to two more times and averaged (i.e., up to 4 replicates). Individual standard curves were used for each plate.

3.1.10. SDS-PAGE/western blot analysis of pS129-α-syn

Twenty-µg total protein per sample of the soluble and insoluble fractions each were fractionated using NuPage 4–12% Bis-Tris gels and the proteins were transferred to 0.2-µm nitrocellulose membranes. Membranes were probed for pS129-α-syn using mAb MJF-R13 [8] (Abcam, ab168381) at a 1:1000 dilution. An HRP-conjugated goat anti-

rabbit secondary antibody (Santa Cruz) was used at a 1:2000 dilution and bands were visualized using HyGLO Quick Spray chemiluminescent detection reagent (Denville, #E2400) and imaged using a Syngene PXi digital imager (Syngene, Frederick, MD). Ponceau S was used as a loading control and α-syn was normalized to the Ponceau-S signal of the entire lane. Finally, the densitometric value of each band was normalized to the total α-syn value in each fraction. Densitometric analysis was performed using ImageJ [37].

3.1.11. Native polyacrylamide gel electrophoresis (NativePAGE) and western blot

The soluble fraction was analyzed using the NativePAGE Novex Bis-Tris Gel System (Invitrogen, Carlsbad, CA) as described previously [38]. Extracts were prepared in a modified NativePAGE sample buffer (50 mM BisTris, 10 mM NaCl, 12% Glycerol, 0.001% Ponceau S, pH 7.2) and a Coommassie Blue G-250 solution (0.02% Coommassie Blue G-250 (VWR) + 75 mM 6-aminohexanoic acid (Sigma-Aldrich)) was added just prior to loading. Ten µg of total protein per well were loaded onto NativePAGE 4-16% Bis-Tris Protein Gels (Invitrogen) and run at 140 V for 110 min, using pre-chilled $1\times$ NativePAGE Light Blue Cathode and Anode Buffers (NativePAGE Running Buffer Kit; Invitrogen) in the inner and outer buffer chambers, respectively, of a XCell SureLock Mini-Cell (Invitrogen). Proteins were transferred onto polyvinyl difluoride (PVDF) membranes (ThermoScientific) using a XCell II Blot Module (Invitrogen) in ice-cold $1\times$ NuPAGE Transfer Buffer (Invitrogen) at 25 V for 60 min. After transfer, membranes were incubated in 8% acetic acid for 15 min, then air dried. Membranes were reactivated in methanol and blocked in 5% non-fat milk in TBS + 0.1% Tween-20 (TBST) for 1 h at room temperature (RT). Membranes then were incubated with anti-α-synuclein mAb MJFR1 (ab138501, Abcam) at 1:20,000 dilution in blocking buffer for 1 h at RT, then with HRP-conjugated Affinipure Goat Anti-Rabbit IgG (111–035-003, Jackson ImmunoResearch Laboratories, Inc., West Grove, PA, USA) at 1:100,000 dilution in blocking buffer for 1 h at RT. Blots were developed with SuperSignal West Dura Substrate (Thermo Scientific) and imaged using an Azure c300 (Azure Biosystems, Dublin, CA, USA) digital imager. Densitometric analysis was performed using ImageJ [37]. The abundance of putative oligomer peaks was quantified using the OD values of the area under each putative oligomer peak and presented as a percentage of the total signal in each lane.

3.1.12. Förster resonance energy transfer (FRET) flow cytometry biosensor cell seeding activity assay

HEK293T biosensor cell lines stably expressing full-length α-syn containing the disease-associated A53T substitution fused to either cyan fluorescent protein (CFP) or yellow fluorescent protein (YFP) were a generous gift from Dr. Marc Diamond (University of Texas Southwestern Medical Center, Dallas, TX). Single-positive cells were used as CFP-only and YFP-only positive controls. Cells were grown in DMEM (Gibco) supplemented with 10% FBS (Nucleus Biologics), 1% PenStrep (Gibco), and 1% GlutaMAX (Gibco) in a humidified incubator at 37 °C and 5% CO₂ atmosphere. For the seeding activity assay, cells were plated at a density of 30,000 cells/well in 96-well plates. Twenty-four hours later (~60% confluency), seed complexes were added. To prepare complexes, soluble-fraction lysate samples were diluted in OptiMem (Gibco) and sonicated for 5 min using a Branson 1510 bath sonicator, then combined with 8.75 µL OptiMEM + 1.25 µL Lipofectamine 2000 (Invitrogen) for a total of 20 µL/well. Seed complexes containing 20 µg total protein/well were incubated at RT for 30 min before being added to cells. Control cells were incubated with the same solution but without brain extracts. After 72 h, cells were harvested with TrpLE (Gibco), transferred to 96-well round bottom plates, fixed in 4% paraformaldehyde (Electron Microcrply Services) in PBS for 10 min, then resuspended in flow-cytometry buffer (1% FBS, 1 mM EDTA in Hanks' Balanced Salt solution). FRET flow cytometry was performed using a BD Biosciences LSR II flow cytometer and FACSDiva

software. To measure CFP and FRET, cells were excited with the 405-nm laser and captured using 405/50-nm and 525/50-nm filters, respectively. To measure YFP, cells were excited with a 488-nm laser and captured using a 525/50-nm filter. CFP spill-over into the YFP and FRET channels was compensated for using CFP-only cells. Following acquisition, flow cytometry data was analyzed using FlowJo v10. Signal within the FRET filter that arises from direct activation of YFP by the 405-nm laser was excluded by introducing a "false FRET" gate, drawn from YFP-only cells. A final triangular FRET gate was made using Lipofectamine-only cells and the background FRET signal was set at ~1%. Cells that shifted into this gate were considered FRET +. The integrated FRET density was defined as the percentage of FRET + cells multiplied by the median fluorescent intensity (MFI), and standardized by dividing the value of Lipofectamine-only control cells. For each experiment, 20,000 single cells per replicate were analyzed and each sample was run in triplicate.

3.1.13. Statistical analysis

All data are presented as mean ± SD or mean ± SEM as appropriate. To test statistical significance of the treatment, the data were analyzed using one-way or two-way ANOVA as appropriate. Correlations between behavioral, histological, and biochemical read-outs were performed by linear regression analysis. Statistical significance was set at $p < 0.05$ considering two-tailed confidence interval. All statistical analyses were performed using GraphPad Prism 7 Software.

Transparency document

The Transparency document associated with this article can be found, in online version.

Declaration of Competing Interest

The authors declare that they have no competing interests.

Acknowledgments

Appendix A. Supplementary data

Supplementary data to this article can be found online at https://doi.org/10.1016/j.bbadis.2019.07.007.

References

[1] A. Fanciulli, G.K. Wenning, Multiple-system atrophy, N. Engl. J. Med. 372 (2015) 249–263.

[2] N. Stefanova, G.K. Wenning, Review: multiple system atrophy: emerging targets for interventional therapies, Neuropathol. Appl. Neurobiol. 42 (2016) 20–32.

[3] S.B. Prusiner, A.L. Woerman, D.A. Mordes, J.C. Watts, R. Rampersaud, D.B. Berry, S. Patel, A. Oehler, J.K. Lowe, S.N. Kravitz, D.H. Geschwind, D.V. Glidden, G.M. Halliday, L.T. Middleton, S.M. Gentleman, L.T. Grinberg, K. Giles, Evidence for alpha-synuclein prions causing multiple system atrophy in humans with parkinsonism, Proc. Natl. Acad. Sci. U. S. A. 112 (38) (2015) E5308–E5317.

[4] F. Bassil, P.O. Fernagut, E. Bezard, A. Pruvost, T. Leste-Lasserre, Q.Q. Hoang, D. Ringe, G.A. Petsko, W.G. Meissner, Reducing C-terminal truncation mitigates synucleinopathy and neurodegeneration in a transgenic model of multiple system atrophy, Proc. Natl. Acad. Sci. U. S. A. 113 (2016) 9593–9598.

[5] L. Fellner, D. Kuzdas-Wood, J. Levin, S. Ryazanov, A. Leonov, C. Griesinger, A. Giese, G.K. Wenning, N. Stefanova, Anle138b partly ameliorates motor deficits despite failure of neuroprotection in a model of advanced multiple system atrophy, Front. Neurosci. 10 (2016) 99.

[6] M. Mandler, E. Valera, E. Rockenstein, M. Mante, H. Weninger, C. Patrick, A. Adame, S. Schmidhuber, R. Santic, A. Schneeberger, W. Schmidt, F. Mattner, E. Masliah, Active immunization against alpha-synuclein ameliorates the degenerative pathology and prevents demyelination in a model of multiple system atrophy, Mol. Neurodegener. 10 (2015) 10.

[7] S. Koga, N. Aoki, R.J. Uitti, J.A. van Gerpen, W.P. Cheshire, K.A. Josephs, Z.K. Wszolek, J.W. Langston, D.W. Dickson, When DLB, PD, and PSP masquerade as MSA: an autopsy study of 134 patients, Neurology 85 (2015) 404–412.

[8] A. Attar, G. Bitan, Disrupting self-assembly and toxicity of amyloidogenic protein oligomers by "molecular tweezers" - from the test tube to animal models, Curr. Pharm. Des. 20 (2014) 2469–2483.

[9] Schrader, T., Bitan, G., and Klarner, F. G. (2016) Molecular tweezers for lysine and arginine - powerful inhibitors of pathologic protein aggregation. Chem. Commun. (Camb.) 52, 11318-11334.

[10] S. Sinha, D.H. Lopes, Z. Du, E.S. Pang, A. Shanmugam, A. Lomakin, P. Talbiersky, A. Tennstaedt, K. McDaniel, R. Bakshi, P.Y. Kuo, M. Ehrmann, G.B. Benedek, J.A. Loo, F.G. Klarner, T. Schrader, C. Wang, G. Bitan, Lysine-specific molecular tweezers are broad-spectrum inhibitors of assembly and toxicity of amyloid proteins, J. Am. Chem. Soc. 133 (2011) 16958–16969.

[11] S. Acharya, B.M. Safaie, P. Wongkongkathep, M.I. Ivanova, A. Attar, F.G. Klarner, T. Schrader, J.A. Loo, G. Bitan, L.J. Lapidus, Molecular basis for preventing alpha-synuclein aggregation by a molecular tweezer, J. Biol. Chem. 289 (2014) 10727–10737.

[12] S. Prabhudesai, S. Sinha, A. Attar, A. Kotagiri, A.G. Fitzmaurice, R. Lakshmanan, M.I. Ivanova, J.A. Loo, F.G. Klarner, T. Schrader, M. Stahl, G. Bitan, J.M. Bronstein, A novel "molecular tweezer" inhibitor of alpha-synuclein neurotoxicity in vitro and in vivo, Neurotherapeutics. 9 (2012) 464–476.

[13] A. Lulla, L. Barnhill, G. Bitan, M.I. Ivanova, B. Nguyen, K. O'Donnell, M.C. Stahl, C. Yamashiro, F.G. Klarner, T. Schrader, A. Sagasti, J.M. Bronstein, Neurotoxicity of the Parkinson's disease-associated pesticide ziram is synuclein-dependent in zebrafish embryos, Environ. Health Perspect. 124 (11) (2016) 1766–1775.

[14] S.M. Fogerson, A.J. van Brummen, D.J. Busch, S.R. Allen, R. Roychaudhuri, S.M. Banks, F.G. Klarner, T. Schrader, G. Bitan, J.R. Morgan, Reducing synuclein accumulation improves neuronal survival after spinal cord injury, Exp. Neurol. 278 (2016) 105–115.

[15] F. Richter, S.R. Subramaniam, I. Magen, P. Lee, J. Hayes, A. Attar, C. Zhu, N.R. Franich, N. Bove, K. De La Rosa, J. Kwong, F.G. Klarner, T. Schrader, M.F. Chesselet, G. Bitan, A molecular tweezer ameliorates motor deficits in mice overexpressing alpha-synuclein, Neurotherapeutics 14 (4) (2017) 1107–1119.

[16] V. Refolo, F. Bez, A. Polissidis, D. Kuzdas-Wood, E. Sturm, M. Kamaratou, W. Poewe, L. Stefanis, C.M. Angela, M. Romero-Ramos, G.K. Wenning, N. Stefanova, Progressive striatonigral degeneration in a transgenic mouse model of multiple system atrophy: translational implications for interventional therapies, Acta Neuropathol. Commun. 6 (2018) 2.

[17] G.G. Kovacs, U. Wagner, B. Dumont, M. Pikkarainen, A.A. Osman, N. Streichenberger, I. Leisser, J. Verchere, T. Baron, I. Alafuzoff, H. Budka, A. Perret-Liaudet, I. Lachmann, An antibody with high reactivity for disease-associated alpha-synuclein reveals extensive brain pathology, Acta Neuropathol 124 (2012) 37–50.

[18] T. Brudek, K. Winge, N.B. Rasmussen, J.M. Bahl, J. Tanassi, T.K. Agander, T.M. Hyde, B. Pakkenberg, Altered alpha-synuclein, parkin, and synphilin isoform levels in multiple system atrophy brains, J. Neurochem. 136 (2016) 172–185.

[19] H. Fujiwara, M. Hasegawa, N. Dohmae, A. Kawashima, E. Masliah, M.S. Goldberg, J. Shen, K. Takio, T. Iwatsubo, Alpha-Synuclein is phosphorylated in synucleinopathy lesions, Nat. Cell Biol. 4 (2002) 160–164.

[20] G. Bitan, E.A. Fradinger, S.M. Spring, D.B. Teplow, Neurotoxic protein oligomers–what you see is not always what you get, Amyloid 12 (2005) 88–95.

[21] D.A. Fancy, T. Kodadek, Chemistry for the analysis of protein-protein interactions: rapid and efficient cross-linking triggered by long wavelength light, Proc. Natl. Acad. Sci. U. S. A. 96 (1999) 6020–6024.

[22] G. Bitan, D.B. Teplow, Rapid photochemical cross-linking–a new tool for studies of metastable, amyloidogenic protein assemblies, Acc. Chem. Res. 37 (2004) 357–364.

[23] D.H. Lopes, S. Sinha, C. Rosensweig, G. Bitan, Application of photochemical cross-linking to the study of oligomerization of amyloidogenic proteins, Methods Mol. Biol. 849 (2012) 11–21.

[24] A. Oueslati, M. Ximerakis, K. Vekrellis, Protein transmission, seeding and degradation: key steps for alpha-synuclein prion-like propagation, Exp. Neurobiol. 23 (2014) 324–336.

[25] B.B. Holmes, J.L. Furman, T.E. Mahan, T.R. Yamasaki, H. Mirbaha, W.C. Eades, L. Belaygorod, N.J. Cairns, D.M. Holtzman, M.I. Diamond, Proteopathic tau seeding

predicts tauopathy in vivo, Proc. Natl. Acad. Sci. U. S. A. 111 (2014) E4376–E4385.

[27] M.J. Benskey, R.G. Perez, F.P. Manfredsson, The contribution of alpha synuclein to neuronal survival and function - implications for Parkinson's disease, J. Neurochem. 137 (2016) 331–359.

[28] T.J. Collier, D.E. Redmond Jr., K. Steece-Collier, J.W. Lipton, F.P. Manfredsson, Is alpha-synuclein loss-of-function a contributor to parkinsonian pathology? Evidence from non-human primates, Front. Neurosci. 10 (2016) 12.

[29] G.G. Calhoon, K.M. Tye, Resolving the neural circuits of anxiety, Nat. Neurosci. 18 (2015) 1394–1404.

[30] J.T.S. Fortuna, M. Gralle, D. Beckman, F.S. Neves, L.P. Diniz, P.S. Frost, F. Barros-Aragao, L.E. Santos, R.A. Goncalves, L. Romao, D.C. Zamberlan, F.A.A. Soares, C. Braga, D. Foguel, F.C.A. Gomes, F.G. De Felice, S.T. Ferreira, J.R. Clarke, C.P. Figueiredo, Brain infusion of alpha-synuclein oligomers induces motor and non-motor Parkinson's disease-like symptoms in mice, Behav. Brain Res. 333 (2017) 150–160.

[31] Balas, M., Balash, Y., Giladi, N., and Gurevich, T. (2010) Cognition in multiple system atrophy: neuropsychological profile and interaction with mood. *J. Neural Transm.* (*Vienna.*) **117**, 369-375.

[32] L.Y. Zhang, B. Cao, Y.T. Zou, Q.Q. Wei, R.W. Ou, B. Zhao, Y. Wu, H.F. Shang, Depression and anxiety in multiple system atrophy, Acta Neurol. Scand. 137 (1) (2017) 33–37.

[33] A. Attar, C. Ripoli, E. Riccardi, P. Maiti, D.D. Li Puma, T. Liu, J. Hayes, M.R. Jones, K. Lichti-Kaiser, F. Yang, G.D. Gale, C.H. Tseng, M. Tan, C.W. Xie, J.L. Straudinger, F.G. Klarner, T. Schrader, S.A. Frautschy, C. Grassi, G. Bitan, Protection of primary neurons and mouse brain from Alzheimer's pathology by molecular tweezers, Brain 135 (2012) 3735–3748.

[34] P.J. Kahle, M. Neumann, L. Ozmen, V. Muller, H. Jacobsen, W. Spooren, B. Fuss, B. Mallon, W.B. Macklin, H. Fujiwara, M. Hasegawa, T. Iwatsubo, H.A. Kretzschmar, C. Haass, Hyperphosphorylation and insolubility of alpha-synuclein in transgenic mouse oligodendrocytes, EMBO Rep. 3 (2002) 583–588.

[35] P. Talbiersky, F. Bastkowski, F.G. Klarner, T. Schrader, Molecular clip and tweezer introduce new mechanisms of enzyme inhibition, J. Am. Chem. Soc. 130 (2008) 9824–9828.

[36] B.B. Holmes, S.L. DeVos, N. Kfoury, M. Li, R. Jacks, K. Yanamandra, M.O. Ouidja, F.M. Brodsky, J. Marasa, D.P. Bagchi, P.T. Kotzbauer, T.M. Miller, D. Papy-Garcia, M.I. Diamond, Heparan sulfate proteoglycans mediate internalization and propagation of specific proteopathic seeds, Proc. Natl. Acad. Sci. U. S. A. 110 (2013) E3138–E3147.

[37] Abramoff, M. D., Magalhaes, P. J., and Ram, S. J. (2004) Image processing with ImageJ.

[38] H. Schagger, W.A. Cramer, von, J. G., Analysis of molecular masses and oligomeric states of protein complexes by blue native electrophoresis and isolation of membrane protein complexes by two-dimensional native electrophoresis, Anal. Biochem. 217 (1994) 220–230.